

Revised SWIRE photometric redshifts

Michael Rowan-Robinson et al

Astrophysics Group, Blackett Laboratory, Imperial College of Science Technology and Medicine, Prince Consort Road, London SW7 2AZ

19 September 2011

ABSTRACT

Key words: infrared: galaxies - galaxies: evolution - star:formation - galaxies: starburst - cosmology: observations

1 INTRODUCTION

To support the Spitzer Hermes submillimetre surveys, we have rerun the methodology of the SWIRE Photometric Redshift Catalogue (SPRC, Rowan-Robinson et al 2008) on the new fusion catalogues supplied by Mattia Vaccari, for the SWIRE areas Lockman, EN1, EN2 and XMM-LSS.

The advent of revised WFC optical fluxes for Lockman, EN1 and EN2 (Gonzalez-Solares et al 2011), the release of CFHT Megacam optical fluxes for XMM (ref), and the UKIDSS DR8 release of J, K magnitudes for Lockman, EN1 and XMM-LSS (ref), make it worthwhile revisiting the SWIRE photometric redshifts in these areas. Rowan-Robinson et al (2008) used optical magnitudes and Spitzer IRAC 3.6 and 4.5 μm fluxes to estimate photometric redshifts. They reported difficulty in incorporating 2MASS and UKIDSS J,H,K magnitudes into the solution, which they attributed to issues of aperture matching. These problems have been solved here. The use of these additional bands, together with the improved optical photometry, has resulted in a reduction in the number of catastrophic outliers and improved rms values, when photometric and spectroscopic redshifts are compared. Since redshifts are now determined from up to 15 bands, compared with generally a maximum of 7 previously, the new redshifts are more reliable. The new catalogues comprise over 700,000 redshifts, out of a total of 1,100,000 in the original SPRC.

The fusion catalogues compiled by Mattia Vaccari (ref) comprise all the available photometric data in the fields surveyed by Spitzer as part of the Hermes survey. TOPCAT was used to merge the SPRC catalogues for Lockman, EN1, EN2 and XMM-LSS with the fusion catalogues, to get the desired photometric data. Not all SPRC sources found matches, mostly

because Spitzer sources detected only at 24 μm were not included in the fusion catalogues.

2 APERTURE CORRECTIONS

Aperture matching between wavelength bands is crucial to the success of photometric redshifts. For distant galaxies photometry in a 2 or 3 arcsec aperture will give the integrated light from the whole galaxy. For nearby galaxies photometry in the same aperture would be dominated by light from the central regions of the galaxy and might comprise only a few % of the integrated light. In template-fitting methods such as we are using here it is natural to try to seek an estimate of the integrated spectral energy distribution (SED), so that near and distant galaxies can be fitted with the same template. This also has the benefit that derived properties such as luminosity, star-formation rate, stellar mass and dust mass have a physical meaning for the galaxy.

There are several options for estimating the integrated light from an extended galaxy in any particular waveband. Optical and near infrared catalogues generally provide Kron and Petrosian integrated magnitudes. SExtractor provides a mag-auto integrated magnitude. These are derived by a curve of growth fitted to photometry derived in a series of apertures of different sizes. However in practice using integrated magnitude estimates for each photometric band to derive the integrated SED gives poor results for photometric redshifts. This is presumably because of the uncertainty introduced by the process of estimating the integrated magnitude. A much more successful option is to start from photometry derived in a single small aperture in each band, and then apply an aperture correction derived in a single chosen band

to all the bands. This is the approach followed by Gonzalez-Solares et al (2011).

2.1 Optical data

The optical photometry in SPRC had been derived in most areas using SExtractor and we used magnitudes measured in a 2" aperture, applying an r-band aperture correction

$$\text{delmag} = r(\text{mag-auto}) - r \quad (1)$$

to all bands. For Spitzer IRAC data we used 'aper-2' fluxes for sources with $\text{area} \cdot 3.6 < 200$, and Kron fluxes for sources larger than this. Fig 1L shows the optical aperture correction, delmag, used in SPRC, versus redshift for the Lockman area. The aperture correction was only applied to the optical magnitudes if it lies in the range -0.10 to -5.0. Otherwise it was set to zero.

For SDSS optical data, available for the Lockman, EN1 and EN2 areas, the 'model' magnitude provides a well-calibrated integrated magnitude. Fig 1R shows delmag versus $r(\text{SDSS,model}) - r(\text{WFC,mag-auto})$. Quasars almost all have no aperture correction, as expected. For galaxies there is no sign of any correlation of $r(\text{SDSS,model}) - r(\text{WFC,mag-auto})$ with delmag, so the SLOAN model magnitude is estimating approximately the same total magnitude as the WFC mag-auto. However there is quite a wide dispersion in $r(\text{SDSS,model}) - r(\text{WFC,mag-auto})$, sufficient to harm photometric redshift estimation (see SED plots below). We have therefore added $r(\text{WFS,mag-auto}) - r(\text{SDSS,model})$ to the SDSS model magnitudes to normalize the two sets of aperture corrections. The reason for making the WFC r-magnitude the preferred choice is that there are far more SWIRE sources with WFC data than with SLOAN data. For SDSS data we investigated using PS magnitudes, with aperture correction $r(\text{SDSS,Petr}) - r(\text{SDSS,PS})$, but this gave inferior results to using the SDSS model magnitudes.

We investigated various other options for aperture corrections in the optical. The revised WFC photometry of Gonzalez-Solares et al (2011), available in the fusion catalogues, includes the Petrosian magnitude in each band, so we define

$$\text{delmag1} = r(\text{WFC,Petr}) - r(\text{WFS,aper2}). \quad (2)$$

This is well correlated with delmag (Fig 2L), but with significant scatter.

Using delmag1 instead of delmag led to slightly worse phot-z results, so we decided to stick with delmag, which was derived from the SExtractor r-band mag-auto, for WFC data (while using the revised WFC magnitudes supplied in the fusion catalogue). However where a mag-auto estimate is not available, we have used delmag1.

2.2 Near infrared data

For UKIDSS data the natural aperture correction to consider is

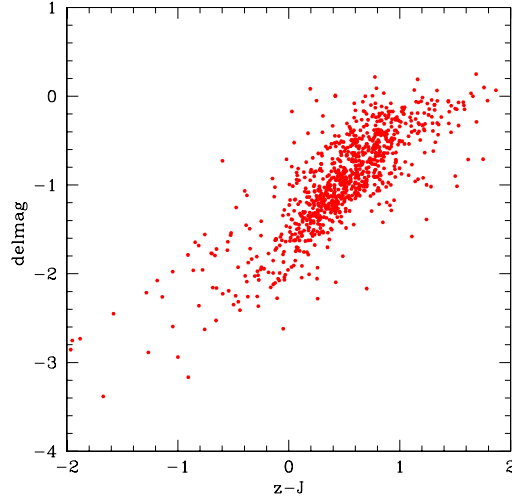


Figure 3. SPRC aperture correction versus $z-J$, with no aperture correction applied to J .

$$\text{delmag3} = K(\text{UKIDSS,Petr}) - K(\text{UKIDSS,aper3}), \quad (3)$$

applied to the aper3 J,K magnitudes. For 2MASS data an option is to use the K-iso magnitude if available, and the K-PS magnitude otherwise, with aperture correction

$$\text{delmag5} = K(2\text{MASS,iso}) - K(2\text{MASS,PS}). \quad (4)$$

Both delmag3 and delmag5 are quite well correlated with delmag (Fig 2R shows the correlation of delmag3 with delmag) and this suggests the idea of using $k \cdot \text{delmag}$ as the near infrared aperture correction, with k to be determined for each survey. The direct use of delmag3 and delmag5 for UKIDSS and 2MASS magnitudes, respectively, resulted in a worse phot-z solution, so the use of $k \cdot \text{delmag}$ was explored in some detail.

Fig 3 shows delmag versus $(z-J)$, with no aperture correction applied to J . There is a very strong correlation. Fig 4L shows delmag versus $(z-J)$ for 2MASS data, with an aperture correction $0.7 \cdot \text{delmag}$ applied to J . Fig 4R shows delmag versus $(z-J)$ for UKIDSS data, with an aperture correction $1.1 \cdot \text{delmag}$ applied to J . We can see that these corrections work well in removing the correlation of colour with delmag.

2.3 IRAC data

In SPRC we used Kron fluxes if the $3.6 \mu\text{m}$ size was greater than a specified threshold, aper2 fluxes otherwise. This is also the approach adopted here. Fig 5 shows delmag versus $(K - \text{am}(3.6 \mu\text{m}))$ for 2MASS (L) and UKIDSS (R) data. There are some residual issues for the UKIDSS-IRAC comparison. Changing the IRAC aperture correction to $k \cdot \text{delmag}$ improved the appearance of Fig 6R enormously, but led to worse phot-z results. The main problem was an offset of the

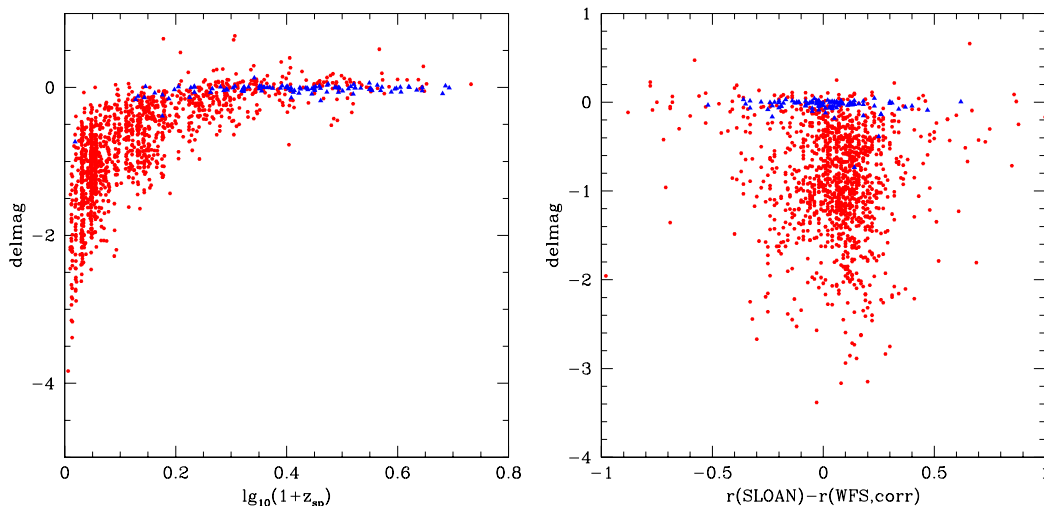


Figure 1. LH: SPRC aperture correction versus z_{sp} for Lockman. RH: SPRC aperture correction versus $r(\text{SDSS,model}) - r(\text{WFC,mag-auto})$.

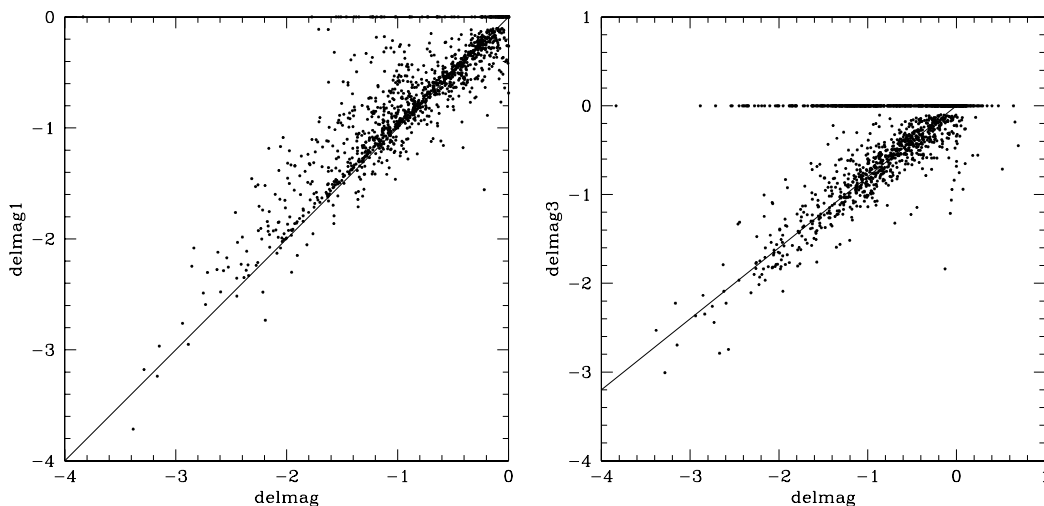


Figure 2. LH: Plot of delmag1 (eqn 2) versus delmag , the SPRC aperture correction, in Lockman. The straight line has slope 1. RH: Plot of delmag3 (eqn 3) versus delmag , the SPRC aperture correction. The straight line has slope 0.8.

$\log_{10}(1+z_{ph})$ points relative to $\log_{10}(1+z_{sp})$ by ~ 0.01 . This was not fixed by the process of in-band correction factors (Ilbert et al 2006), and it would probably be necessary to revise the templates in the near infrared to achieve convergence.

3 PHOTOMETRIC REDSHIFTS

In the photometric redshift solution we used the new SLOAN 'model' magnitudes, and the revised WFC magnitudes, but we retained the WFC star/galaxy classification in each band and the optical aperture correction used in SPRC. We used 2MASS JHK

(PSC), where available, and UKIDSS JK (aper3) if not.

We used galaxies with known spectroscopic redshifts to determine in-band correction factors, following Ilbert et al (2006).

JHK magnitudes, and 3.6 and 4.5 μm fluxes were used in the solution provided there was no evidence of a strong dust torus [determined by condition $S(5.8) > 1.2 S(3.6)$ on first pass through data, and by dust torus component dominant at 8 μm from ir template fitting on second pass].

Fig 6 shows a comparison of the SLOAN $\log_{10}(1+z_{phot})$ with $\log_{10}(1+z_{spect})$ for the SWIRE Lockman sample (LH). and the same plot for the present sam-

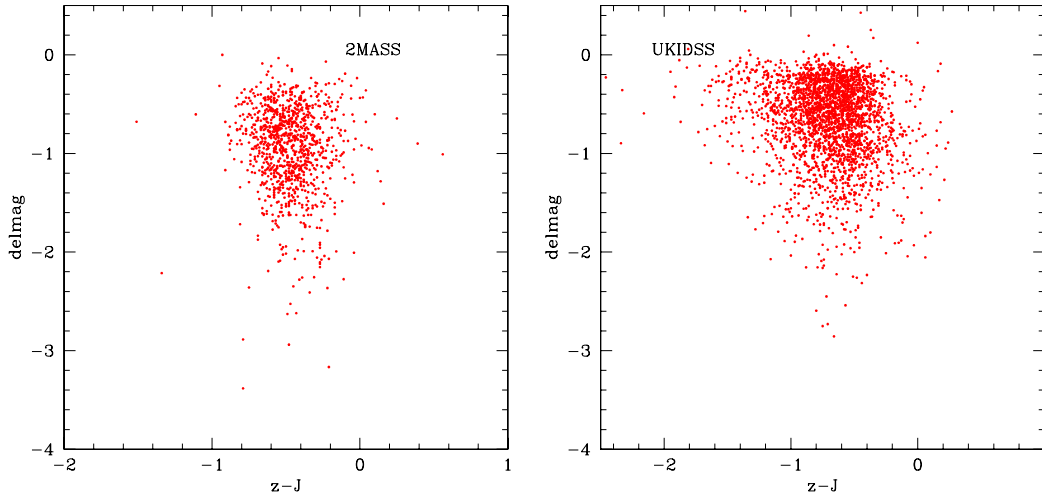


Figure 4. LH: SPRC aperture correction versus corrected ($k=0.7$) $z-J$ for 2MASS. RH: SPRC aperture correction versus corrected ($k=1.1$) $z-J$ for UKIDSS.

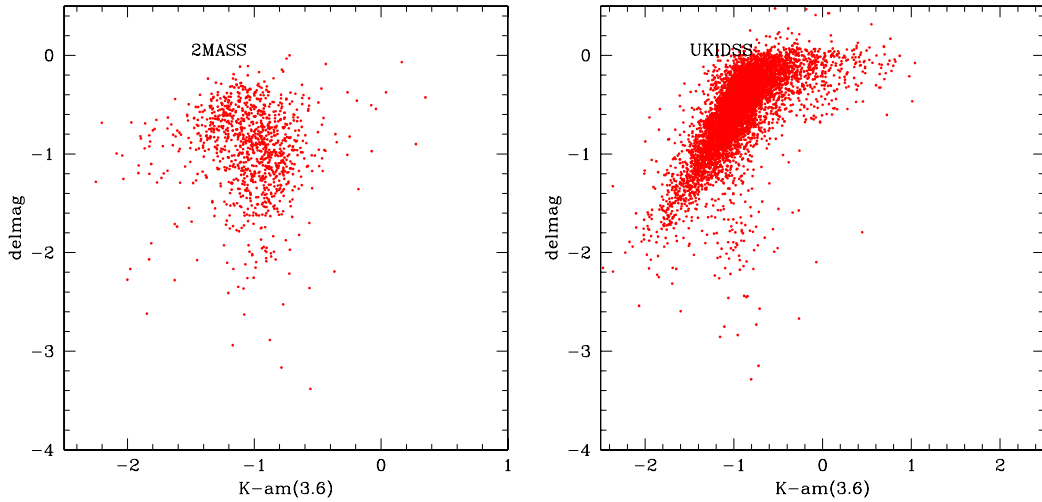


Figure 5. LH: SPRC aperture correction versus corrected ($k=0.7$) $K-am(3.6)$ for 2MASS. RH: SPRC aperture correction versus corrected ($k=1.1$) $K-am(3.6)$ for UKIDSS.

ple (RH). The SDSS performance is better at $z < 0.3$, but our approach works better at $z > 0.5$. To improve our photometric redshifts at $z < 0.3$ it may be necessary to refine our optical templates using the new photometric data. It may also be an issue that we are using only six independent galaxy templates in the optical.

Fig 7L shows the same comparison for the SWIRE Photometric Redshift Catalogue, restricted to $r < 23.5$, reduced $\chi^2 < 3$ and at least 5 photometric bands in the solution. Fig 7R shows a similar plot for the revised SPRC, with the requirement that K be selected, and for a minimum of 7 photometric bands.

We can see that inclusion of near infrared (JHK) data in the solution has improved the outlier rejection.

Fig 8L shows the same comparison for the revised catalogue in XMM, with at least 9 bands in the solution in the solution, compared. Fig 8R shows the same comparison for photometric redshifts from the LePhare method (Ilbert et al 2006). The latter results are better for $z < 0.5$, but worse for $z > 0.5$.

4 QSOS

The SPRC approach requires that an object be flagged as stellar to consider a QSO optical template.

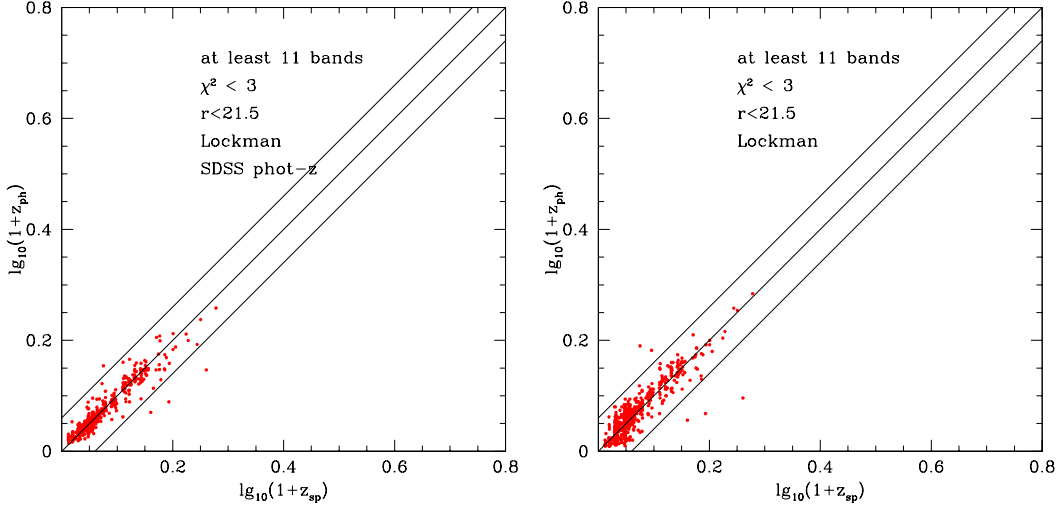


Figure 6. LH: SDSS photometric redshifts versus spectroscopic redshifts for Lockman SWIRE sample. RH: photometric redshifts from present work versus spectroscopic redshifts for Lockman SWIRE sample.

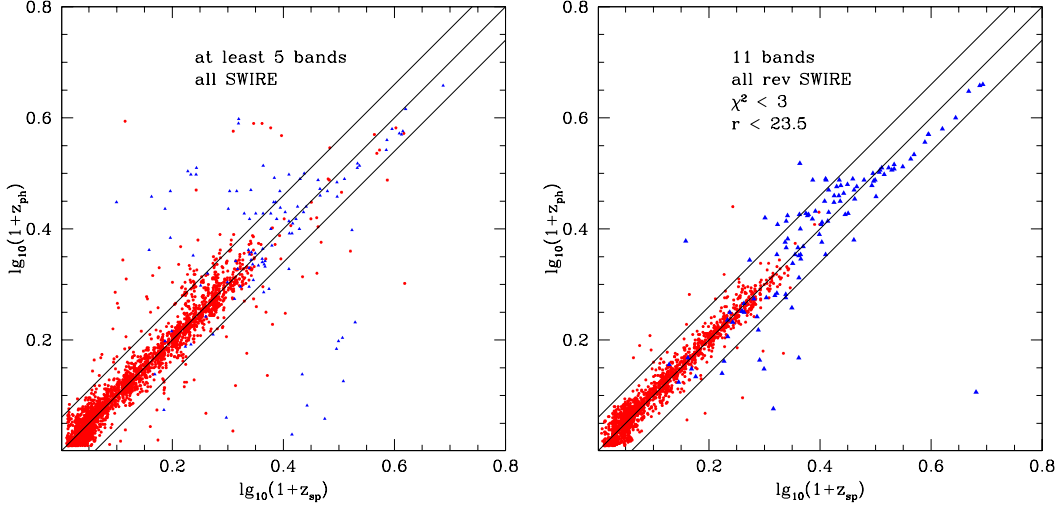


Figure 7. LH: Photometric redshifts from SWIRE Photometric Redshift Catalogue (Rowan-Robinson et al 2008). $r < 23.5$, at least 5 photometric bands, reduced $\chi^2 < 3$. Red symbols: galaxies, blue symbols: QSOs. RH: Same for revised SPRC, with at least 11 photometric bands.

With the SPRC stellar flag some QSOs get missed (and end up with the wrong redshift) as a result of this condition. As discussed in SPRC it is not possible to allow a QSO template option for all galaxies, since far too many galaxies end up with mistakenly high redshifts. However we have allowed the SDSS stellar flag to override the WFS flag where they disagree and this allows a few more quasars through.

Salvato et al (2009) have demonstrated excellent performance for 1032 QSOs and AGN in the COSMOS field, using 30 photometric bands, including 12 narrow-band filters. They introduce two innovations: firstly they track the variability of quasars and ap-

ply an appropriate correction to the photometry. Secondly they use templates that include a range of contributions from AGN dust tori.

While we do not have the information to track QSO variability in our photometry, we have explored the idea of adding a range of AGN dust tori strengths to our templates, and then using the $1.25\text{-}8\ \mu\text{m}$ data in the redshift solution. The amplitude of dust tori added corresponded to $L_{\text{tor}}/L_{\text{opt}} = 0, 0.2, 0.4, 0.6, 0.8, 1.0$. The performance for QSOs is much improved (Fig 7), especially the outlier rejection. For at least 11 photometric bands, reduced $\chi^2 < 3$, $r < 21.5$, we find an rms of 9.3% and an outlier rate 9.3%. For compar-

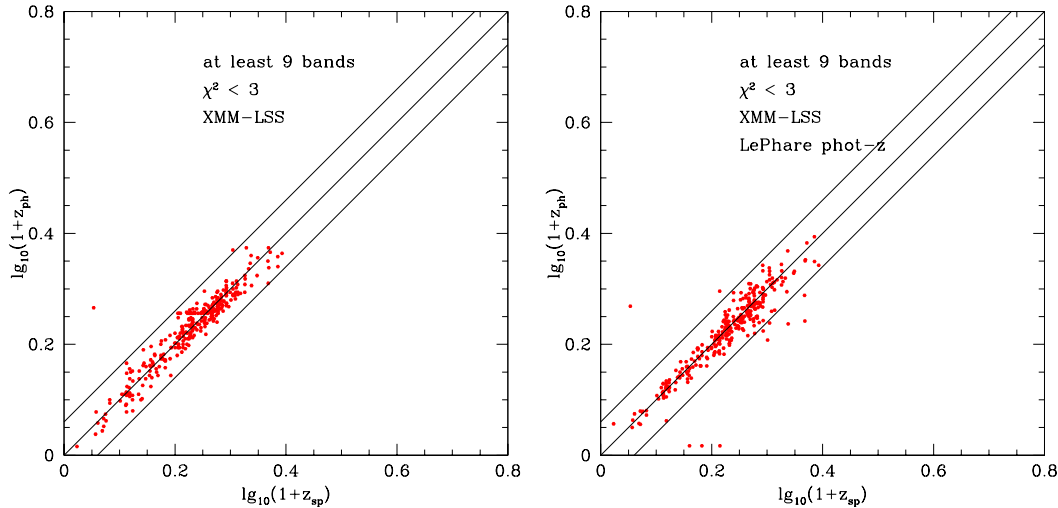


Figure 8. L: Photometric redshifts in XMM-LSS using new fusion catalogue: ugriz from SLOAN, revised ugriz from WFS, JHK from 2MASS, JK from UKIDSS. R: Photometric redshifts from LePhare method (Ilbert et al 20**).

ison, Salvato et al (2009), with 30 bands, achieved an rms of 1.2% for QSOs with $I < 22.5$, and an outlier rate of 6.3%. Their greatly improved rms can be attributed to the correction for variability and to the use of 30 photometric bands, including 12 narrow band filters. Our new catalogue delivers photometric redshifts for 36554 quasars.

5 REVISED SWIRE PHOTOMETRIC REDSHIFT CATALOGUE

Our revised SPRC contains 835410 objects, 209696 in EN1, 117845 in EN2, 220472 in Lockman, and 287397 in XMM-LSS, compared with 875353 in the same areas in the original SPRC. 3.6% of SPRC sources did not find a match in the fusion catalogues, mainly because the latter omitted 24 μm only sources. A further 1% failed to achieve a redshift solution, either because there were less than two valid photometric bands or because the reduced $\chi^2 > 100$. The SWIRE redshifts in CDFS and S1 have not been revised because we have no new photometric information in these areas. These two areas bring the total number of redshifts in the revised catalogue to 1026933 (<http://astro.ic.ac.uk/mrr/swirephotzcat/zcatrev12ff2.dat.gz>, with readmeSWIRErev in same directory).

6 SEDS OF OUTLIERS

To investigate outliers, we have plotted the SEDs of 8 outliers from the z_{phot} v. z_{spec} comparisons in Fig 9 (those with $\chi^2 < 3$, and with more than 12 photometric bands in EN1, EN2 and Lockman, and with more

than 9 bands in XMM-LSS). SLOAN photometry (after applying the aperture correction of section 2.1) is shown in red. Two have aliases at the spectroscopic redshift, one appears to need an Sab template with $A_V = 0.35$ (A_V is set to zero for the Sab template in our code), and 5 could be errors in the spectroscopic redshift (two were based on a single line).

7 DISCUSSION

With the changes discussed in the previous sections, we now see improvements in the rms and outlier rejection for photometric redshifts.

For galaxies with reduced $\chi^2 < 3$, $r < 23.5$, the rms in $(z_{\text{phot}} - z_{\text{spec}})/(1 + z_{\text{spec}})$, after rejection of outliers with values discrepant by 15% or more, is 3,7, 3.4 %, for no. of bands 10, 14 respectively. The corresponding percentages of outliers are 1.2 and 0.2 %, respectively. Fig 14L shows how the percentage of outliers for galaxies with $|\log_{10}(1 + z_{\text{phot}})/(1 + z_{\text{spec}})| > 0.06$, vary with the number of photometric bands. Fig 14R shows the percentage rms ($\sigma_z/(1 + z)$) versus number of photometric bands. The additional photometric bands provided by the JHK data from 2MASS and UKIDSS now have a clear beneficial effect, especially on the outlier rejection. Our results can be compared directly with the corresponding results for SPRC, and with new results from GOODS-S (Daklen et al 2010), and COSMOS30 (Ilbert et al 2009).

REFERENCES

- Daklen T. et al, 2010, ApJ 724, 425
 Gonzalez-Solares E. et al, 2011, MNRAS
 Ilbert O. et al, 2006, AA 457, 8411

Table 1. z_{ph} v. z_{sp} outliers whose SEDs are plotted in Fig 9, from bottom

RA	dec	z_{spec}	ref.	z_{phot}	no. of bands	notes
161.30797	58.74822	0.2470	1	0.52	12	alias
161.72533	58.99032	0.1890	1	0.55	12	alias
161.74496	58.94529	0.8220	1	0.25	12	zspec error ?
161.88536	59.15305	0.4470	2	0.14	13	zspec error ?
161.94997	59.29018	0.5600	2	0.17	13	zspec error ?
36.40352	-4.39069	0.1307	3	0.85	9	zspec error (single line) ?
36.47719	-4.36419	0.8277	3	1.24	9	zspec error (single line) ?
248.47900	41.48283	0.1592	4	0.47	14	need Sab with $A_v=0.35$

1 Owen et al 2009
 2 Rowan-Robinson et al 2008
 3 Le Fevre et al 2005
 4 Rowan-Robinson et al 2004

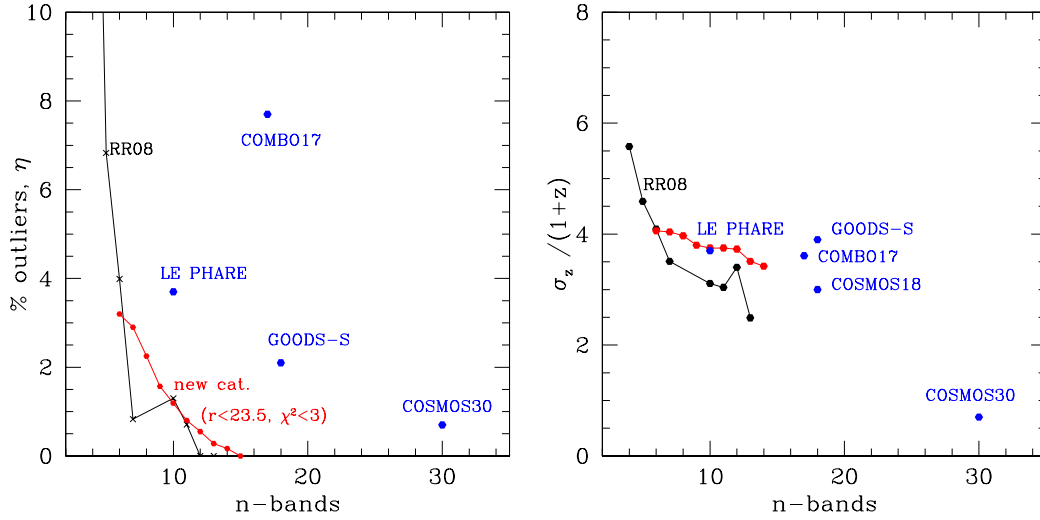


Figure 10. L: Percentage of outliers versus number of photometric bands for SPRC (black loci) and for fusion catalogue (red loci), for sources with reduced $\chi^2 < 3$, $r < 23.5$. R: Percentage rms ($\sigma_z / (1+z)$) for SPRC (black loci) and for fusion catalogue (red loci), for sources with reduced $\chi^2 < 3$, $r < 23.5$.

Ilbert O. et al, 2009, ApJ 609, 1236
 Rowan-Robinson M. et al, 2004, MNRAS 351, 1290
 Rowan-Robinson M. et al, 2008, MNRAS 386, 687
 Salvato M. et al, 2009, ApJ 690, 1250
 Vacari M. et al, 2011, fusion catalogue

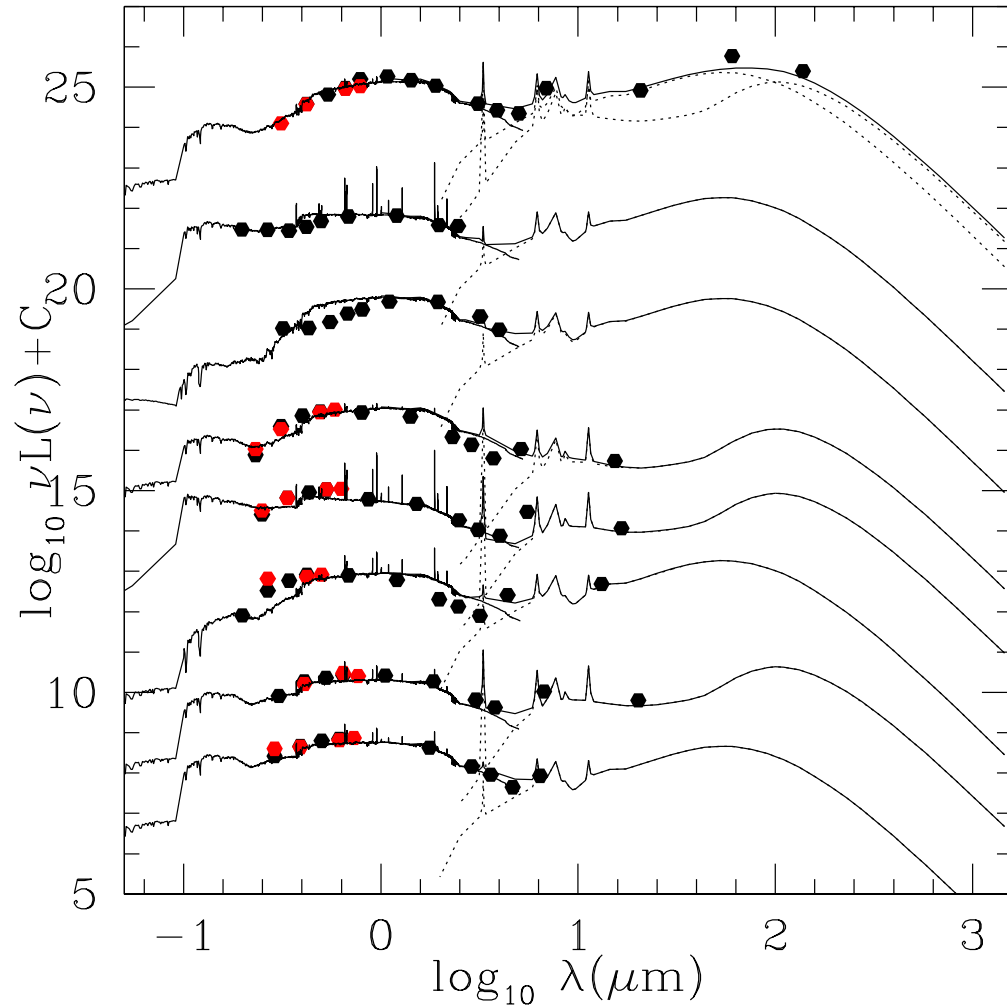


Figure 9. SEDs of outliers in z_{ph} v. z_{sp} plot, with details of sources given in Table 1. Outliers with more than 12 photometric bands in EN1, EN2, Lockman, and more than 9 bands in XMM-LSS, are included.